

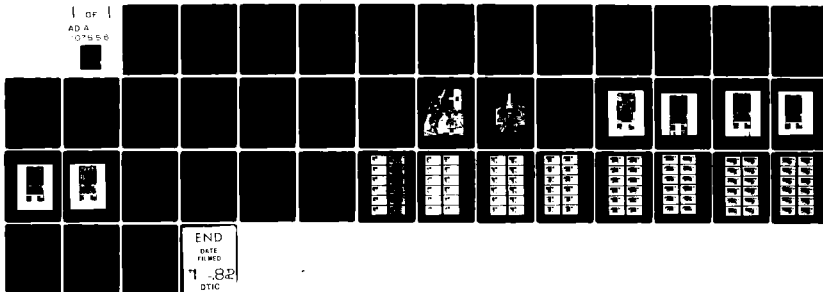
AD-A107 856

NAVAL ACADEMY ANNAPOLIS MD DIV OF ENGINEERING AND WEAPONS F/G 21/7
TIME DEPENDENT ANALYTICAL AND OPTICAL STUDIES OF HEAT BALANCED --ETC(U)
NOV 80 A A POURING, B H RANKIN
USNA-EW-13-80

UNCLASSIFIED

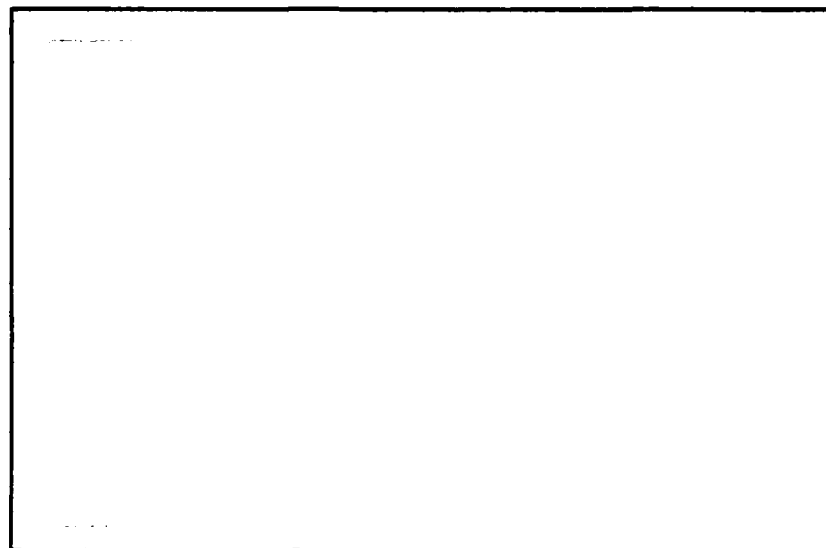
NL

OF
AD A
07/58



AD A107856

10



UNITED STATES NAVAL ACADEMY
DIVISION OF
ENGINEERING AND WEAPONS
ANNAPOLIS, MARYLAND

THIS FILE COPY

NOV 25 1981

A

84 11 24 1982

Time Dependent Analytical and Optical
Studies of Heat Balanced Internal
Combustion Engine Flow Fields

Andrew A. Pouring, Professor
Bruce H. Rankin, Professor

United States Naval Academy
Annapolis, Maryland

November 1980

Report No. EW-13-80



Work sponsored by Power Branch, Code 473, Office of Naval Research

UNCLASSIFIED

SECURITY CLASSIFICATION OF THIS PAGE (When Data Entered)

REPORT DOCUMENTATION PAGE		READ INSTRUCTIONS BEFORE COMPLETING FORM
1. REPORT NUMBER USNA-EW-13-80	2. GOVT ACCESSION NO. DA-101 102	3. RECIPIENT'S CATALOG NUMBER
4. TITLE (and Subtitle) Time Dependent Analytical and Optical Studies of Heat Balanced Internal Combustion Engine Flow Fields		5. TYPE OF REPORT & PERIOD COVERED Progress, 1977-1980
		6. PERFORMING ORG. REPORT NUMBER EW-13-80
7. AUTHOR(s) A. A. Pouring, Professor B. H. Rankin, Professor		8. CONTRACT OR GRANT NUMBER(s) N0001480WR00156
9. PERFORMING ORGANIZATION NAME AND ADDRESS U. S. Naval Academy Aerospace Engineering Department Annapolis, Maryland 21402		10. PROGRAM ELEMENT, PROJECT, TASK AREA & WORK UNIT NUMBERS
11. CONTROLLING OFFICE NAME AND ADDRESS Office of Naval Research Power Branch, Code 473 Washington, D. C.		12. REPORT DATE November 1980
14. MONITORING AGENCY NAME & ADDRESS (if different from Controlling Office)		13. NUMBER OF PAGES
		15. SECURITY CLASS. (of this report) UNCLASSIFIED
15a. DECLASSIFICATION/DOWNGRADING SCHEDULE		
16. DISTRIBUTION STATEMENT (of this Report) Distribution Unlimited		
17. DISTRIBUTION STATEMENT (of the abstract entered in Block 20, if different from Report)		
18. SUPPLEMENTARY NOTES		
19. KEY WORDS (Continue on reverse side if necessary and identify by block number) Internal Combustion Engines Transient Combustion (Nonsteady) Schlieren photography Fastex cine		
20. ABSTRACT (Continue on reverse side if necessary and identify by block number) Comparison is made of the nonsteady combustion and flow processes pre- dicted by the method of characteristics for time dependent compressible flow in a heat balanced engine with photographic records of combustion flow fields observed by high speed Fastex Schlieren and holographic interferometry. Pressure exchange and the accompanying mass transport are demonstrated analytically and observed optically. Qualitative agreement between the initial top dead center calculation and photographic evidence is seen.		

DD FORM 1 JAN 73 1473

EDITION OF 1 NOV 65 IS OBSOLETE
S/N 0102-014-6601

UNCLASSIFIED

SECURITY CLASSIFICATION OF THIS PAGE (When Data Entered)

UNCLASSIFIED

SECURITY CLASSIFICATION OF THIS PAGE (When Data Entered)

19. (Cont'd)

Interferometry

Holography

Time dependent characteristics analysis

Combustion Waves

Naval Academy Heat Balanced Engine (NAHBE)

Pressure exchange

Time dependent compressible flow

20. (Cont'd)

Schlieren and interferometer records give typical combustion flow field interactions through all strokes of an operating four stroke glass walled two dimensional engine. At least four modes of time dependent combustion are identified over the entire power stroke and the influence of geometry on the control of combustion chamber pressure and temperature is discussed.

UNCLASSIFIED

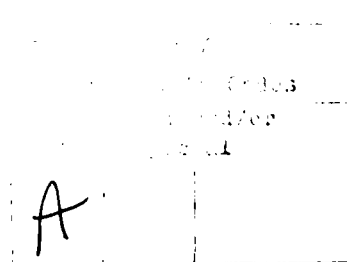
SECURITY CLASSIFICATION OF THIS PAGE (When Data Entered)

TABLE OF CONTENTS

I. Abstract	1
II. Introduction	2
III. Theoretical Nonsteady Combustion and Flow Fields	4
IV. Experimental Observations - Holographic Interferometry	8
V. Experimental Observations - Fastex Schlieren Photography	11
VI. Conclusions	14
VII. References	16

ACKNOWLEDGEMENT

This work has been made possible by the contributions of many; among them are Dr. Barry Hannah and Lawton King of NSWC, White Oak, Maryland; Earl Krabill, the Trident Scholars and other student researchers at the U. S. Naval Academy whose papers are cited as researchers; Dr. Joseph V. Foa, George Washington University, and the support of the Power Branch, ONR, when it was needed most.



TIME DEPENDENT ANALYTICAL AND OPTICAL
STUDIES OF HEAT BALANCED INTERNAL
COMBUSTION ENGINE FLOW FIELDS

Andrew A. Pouring, Professor
Bruce H. Rankin, Professor

United States Naval Academy
Annapolis, Maryland

I. ABSTRACT

Comparison is made of the nonsteady combustion and flow processes predicted by the method of characteristics for time dependent compressible flow in a heat balanced engine with photographic records of combustion flow fields observed by high speed Fastex Schlieren and holographic interferometry. Pressure exchange and the accompanying mass transport are demonstrated analytically and observed optically. Qualitative agreement between the initial top dead center calculation and photographic evidence is seen. Schlieren and interferometer records give typical combustion flow field interactions through all strokes of an operating four stroke glass walled two dimensional engine. At least four modes of time dependent combustion are identified over the entire power stroke and the influence of geometry on the control of combustion chamber pressure and temperature is discussed.

II. INTRODUCTION

The concept of "heat balancing" in internal combustion engines stems from 2 stage heat addition in a quasi-equilibrium combined (constant volume - constant pressure) cycle⁽¹⁾. It has been shown that the quasi-equilibrium cycle yields output greater than the Otto cycle; while allowing system equilibrium yields the classical combined cycle result with less output than the Otto cycle⁽²⁾. These concepts, of course, are for the theoretical limiting air standard case. It has been proposed⁽³⁾ that the real engine approach for attainment of the benefits of the heat balanced cycle involves combustion with pressure exchange, or the transfer of energy by interface pressure forces.

To better understand the interactions leading to pressure exchange postulated earlier⁽³⁾, a preliminary non-steady gas dynamic analysis⁽⁴⁾ was conducted with the conclusion that, even for the top dead center stationary piston boundary condition considered, pressure exchange was possible with the attendant enhancement of combustion from balancing chamber air transported to the combustion front. The present study compares the earlier non-steady time dependent method of characteristics results⁽⁴⁾ with those of several optical techniques of observation of combustion in an operating square piston engine designed specifically for 2-dimensional optical flow studies.

The earlier theoretical studies on the heat balanced cycle^(1,2) dealt specifically with limits obtainable according to the laws of thermodynamics. It is important to separate these equilibrium or quasi-equilibrium thermodynamic air standard predictions of an ideal model from the real engine, which in this case is highly non-equilibrium and time dependent in nature. This study therefore deals primarily with real engine processes.

Excellent reviews of the state of the art in time dependent modeling of reciprocating engine processes are given in current literature^(6,7). Although

the numerical methods described are capable of giving velocity and temperature fields at a given instant, they cannot give, at present, continuous interface motion which is of major importance here and an inherent property of the characteristics calculation methods. Also, in contrast to earlier cinematographic Schlieren studies in a single stroke machine⁽⁶⁾, the current work described is from an operating single cylinder, 2 dimensional square bore engine with glass sidewalls^(8,9).

III. THEORETICAL NONSTEADY COMBUSTION AND FLOW FIELDS

A preliminary investigation into the nonsteady aspects of real engines operating on the heat balanced principle was conducted by one of us (AAP) with Professor J. V. Foa, and R. P. Pandalai, graduate student, both of George Washington University⁽⁴⁾. Both frontal and volume modes of combustion were examined on a preliminary basis; only the former will be reviewed here.

The amount of work in calculating a nonsteady characteristics network by hand is considerable so only the top dead center position is considered. Also, heat transfer from the surfaces is not taken into account in the calculation, though known to be important.

A "frontal" mode of combustion is assumed in the preliminary non-steady flow analysis wherein it is assumed that the chemical reactions take place instantaneously as the unburned gas passes through an advancing flame front. This approach considerably reduces the procedures involved in the construction of the wave diagrams on either side of the flame front. The main objective of the construction of the wave diagram is to get an immediate "feel" for the nature and type of interactions and transients involved and their relative strengths. Also one can approximately compute the combustion time which plays an important role in the nature and formation of the combustion products.

Fig. III-1 shows the analytical model used in this non-steady idealized flow analysis. As shown in Figure III-1, region 1, the combustion chamber, is occupied by the combustible mixture, region 2 by the balancing chamber gas (Air). Initially the interface which merely separates the combustible mixture from the air is assumed to be located very close to the balancing chamber at the beginning of ignition. As long as the interface is not reached by the flame front, the state of the gas is the same on either side.

This combustion differs from that of conventional spark ignition combustion because of the presence of a secondary chamber called the balancing

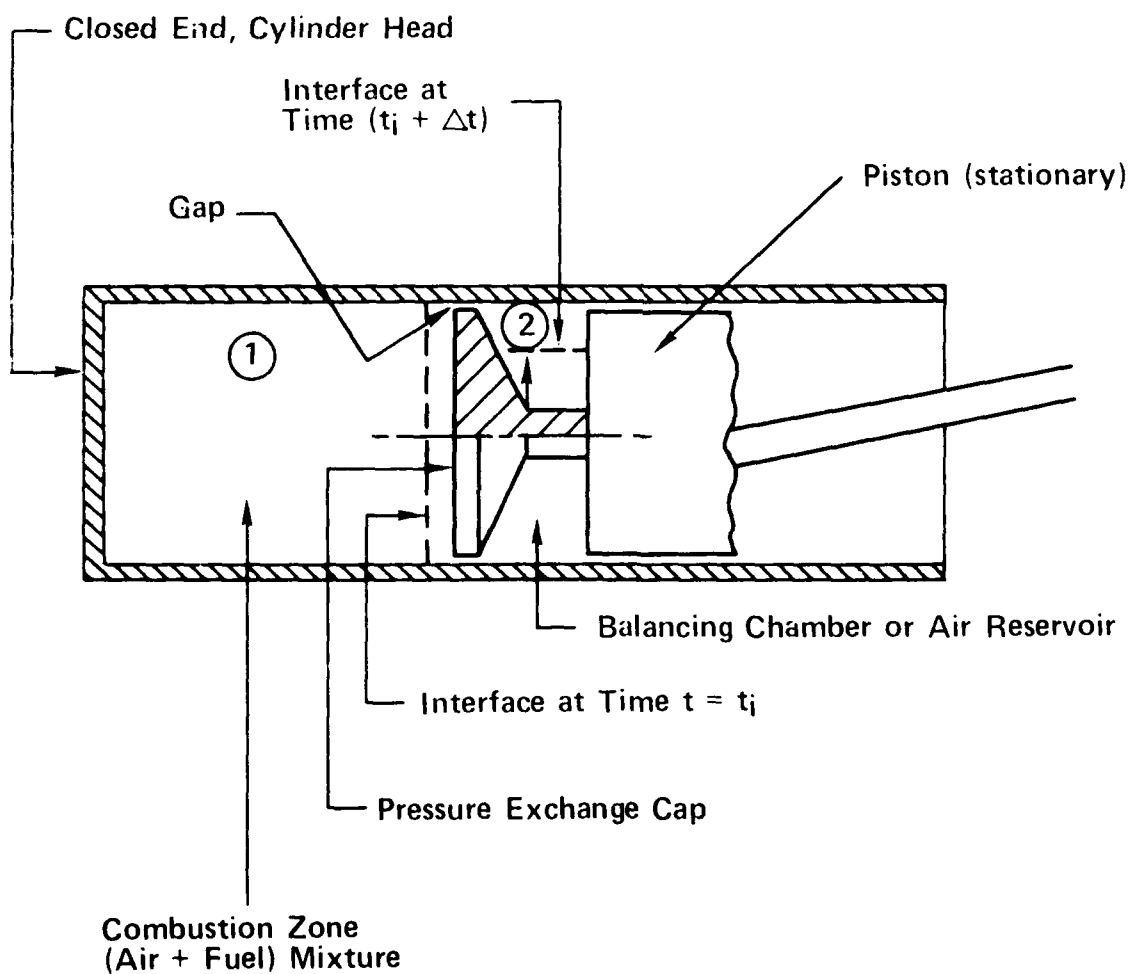


FIGURE III-1
ANALYTICAL MODEL FOR NONSTEADY FLOW ANALYSIS.

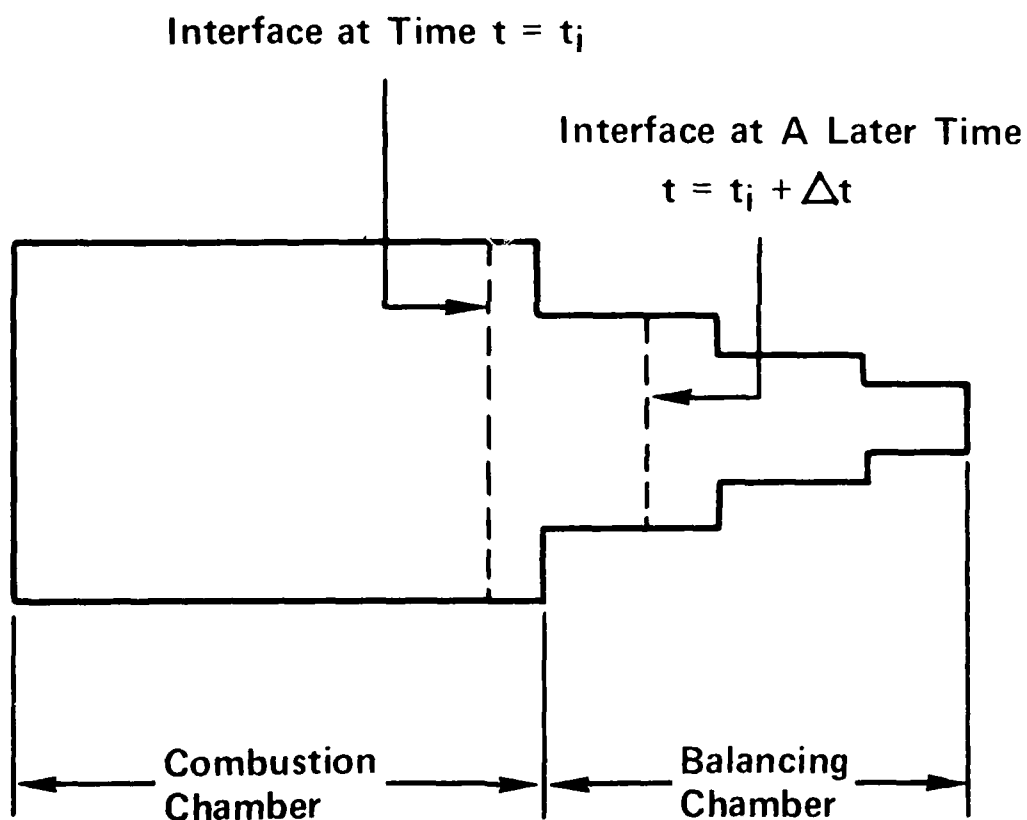


FIGURE III-2 MOVEMENT OF THE INTERFACE DURING COMBUSTION (IDEALIZED ONE DIMENSIONAL SITUATION).

chamber. Reference 3 points out the fact that little or no combustion has been observed in the balancing chamber which merely acts as a reservoir of hot compressed air. According to the pressure exchange mechanism proposed therein, the balancing chamber air is fed into the combustion chamber during the combustion cycle as a result of wave interactions and thereby the combustion proceeds to completion over a longer period of time. Therefore, the movement of the interface and the resulting interactions are of great importance to an understanding of this combustion process.

The plane circular interface after reaching the balancing chamber moves as a cylindrical interface in a conical tube with a gradual reduction in the surface area of the interface. This gradual change in area can be idealized as a finite number of discrete change in area for the purpose of constructing the details of the interactions on a wave diagram. This stepped area is shown in Figure III-2, idealized as a one dimensional process.

Once ignition of the mixture occurs at the closed end, a flame front is produced and advances into the unburned mixture. Since the flame is assumed to reach its burning velocity instantly upon ignition, the acceleration of the gas takes place through a weak shock wave traveling ahead of the flame front. This results in a series of interactions and transients which include:

- (1) The shock wave generated at the closed end interacts with the first discontinuous change of cross section.
- (2) Deflection of the interface by the reflected shock wave at the first change of cross section.
- (3) Interaction of the transmitted shock wave at the second change of cross section, etc.

The interactions and transients that subsequently follow are shown in the wave diagram of Figure III-3.

The following assumptions are made in the non-steady flow analysis:

- (a) The flame front advances into the unburned gas with a burning velocity that is taken proportional to the absolute temperature of the unburned gas.
- (b) Initial air/fuel ratio = α = 20.
- (c) Initial temperature of the mixture = 1200° R.
[This corresponds to an adiabatic compression ratio of 8].
- (d) Changes of pressure and specific heat ratio across the flame front are neglected.
- (e) The motion of the piston during the initial combustion processes is negligible.
- (f) Engine dimensions are for CFR engines³.

Construction of the wave diagram in dimensionless time-distance coordinates is based on standard methods given in references (10) and (11) with detailed calculations in Ref. 4. The movement of the interface with respect to time as combustion proceeds is shown by the dotted lines on the wave diagram. After a certain time, the flame front and the interface interact and reaction is prolonged with the additional oxygen supplied.

ANALYSIS OF THE WAVE DIAGRAM

It is interesting to note that the strength of the initial shock wave characterized by the shock Mach number is comparatively low ($M_s = 1.247$) for the assumed typical initial conditions. The result of the computations is given in Figs. III-3-6 with the pressure ratios and velocities computed for the various regions located on the wave diagram, Fig. III-3.

It is clearly seen from Figure III-3 that once the interface reaches the balancing chamber, the reflected waves from previous interactions moving in the opposite direction towards the combustion chamber slow down the interface and

after some time the interface itself starts moving back towards the combustion chamber. Because the reflected shock waves are all of comparatively small Mach numbers (in the neighborhood of 1.1), the effect of the interaction of these waves on the flame front itself is negligible. However, towards the end of the initial combustion process the flame front is appreciably slowed down by the expansion waves. Finally when the flame front and interface interact, secondary combustion begins and piston motion becomes significant. For this specific case the time for interface-flame front interaction is found to be of the order of 0.15 millisecond.

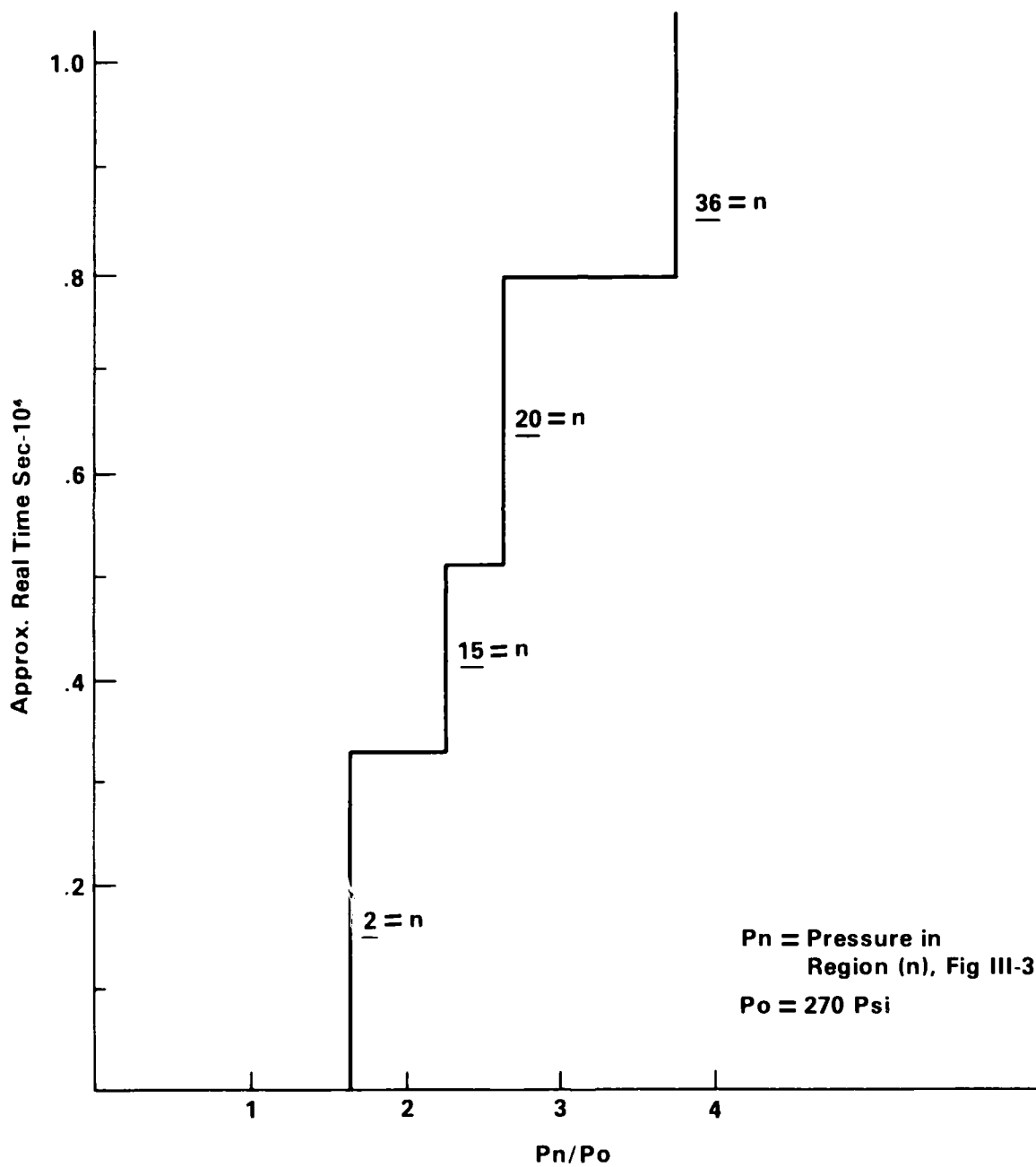


FIGURE III-4

PRESSURE PROFILE AT $\xi = 0.0$ (CYLINDER HEAD)

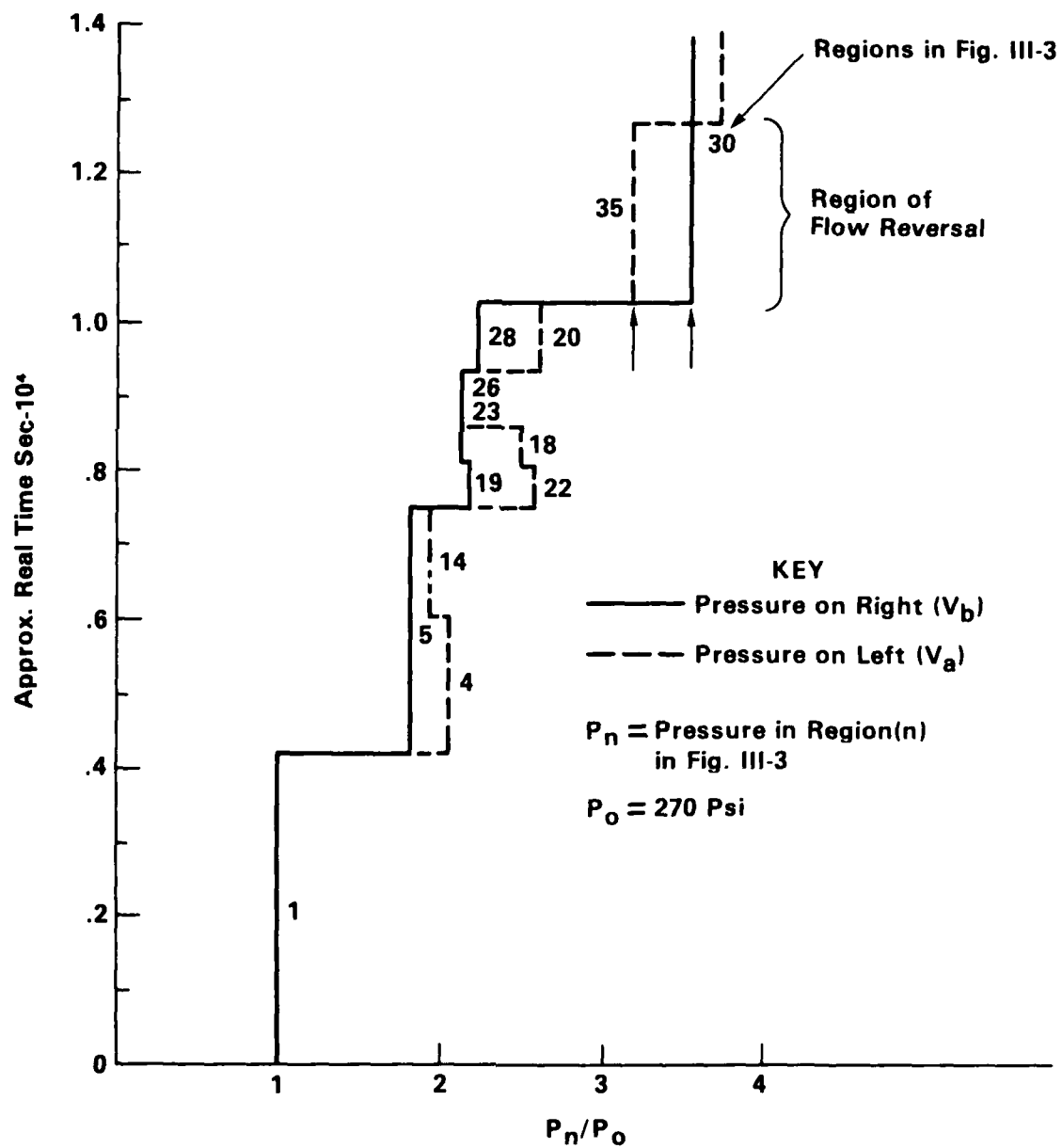


FIGURE III-5

PRESSURE PROFILE AT $\zeta = 1.0$ (CAP LOCATION)

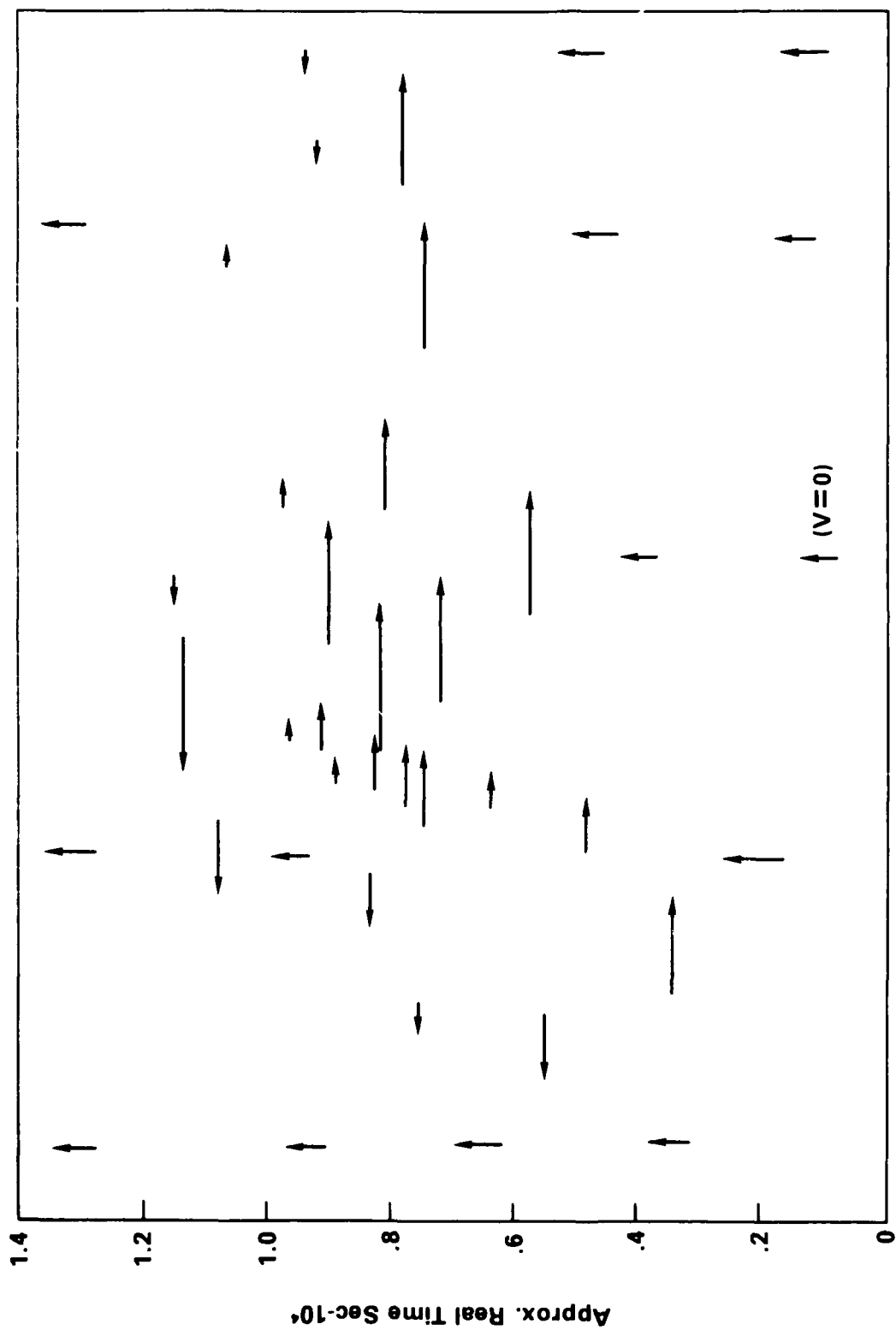


FIGURE III-6

FLOW VELOCITY

IV. EXPERIMENTAL OBSERVATIONS - HOLOGRAPHIC INTERFEROMETRY

The same 2-dimensional square engine with glass (fused silica) sidewalls described elsewhere^(8,9) was used for the interferometry study. Briefly, the engine characteristics (modified Megatech) are:

Bore: 1.625" (4.127 cm)

Stroke: 2.0" (5.08 cm)

Balancing ratio: 0.5

Compression ratio: 2.8

RPM: 1000

Gap clearance: 0.0625" (0.158 cm)

Gap length: 0.100", 0.300" (.254 cm, .762 cm)

Fuel: propane

As seen in Figures IV-1-2, different gap lengths were used on the cap in order to observe their effect on quenching. Details on the two-plate holographic interferometer are given in Refs. 12.

Typical results from the interferometer are given in Figs. IV-3-8 for piston locations from top dead center, $\theta = 0$, to near bottom dead center, $\theta = 180^\circ$. At top dead center (TDC), Fig. IV-3, the combustion front initiated by spark ignition at $\theta \approx -12^\circ$, has developed with a weak wave preceding the combustion kernel, the upper right hand side of the wave gives a fringe shift typical of weak shock waves while the rest of the compression wave is of lower strength. The near horizontal fringes evident ahead of the wave indicate quite uniform, non-turbulent mechanical compression of the combustible gases by the piston. Due to increased flow resistance in the longer gap, flow into the right hand balancing chamber is still evident while the left side is nearly complete.

Fig. IV-4 is at 10° after top dead center (ATDC), or at 1000 RPM, 1.6 msec

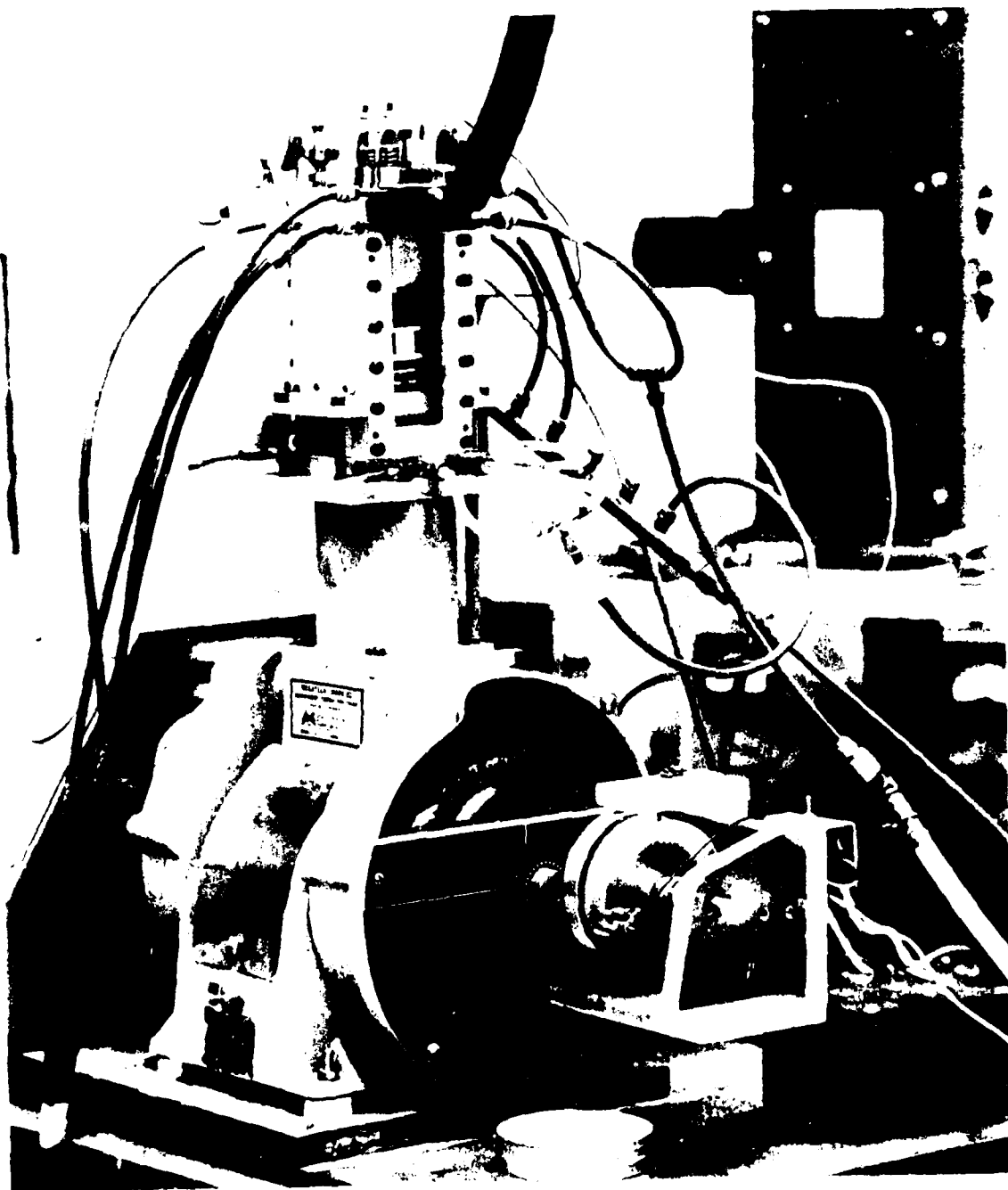


Figure IV-1

Overall View of 2-Dimensional Square Engine

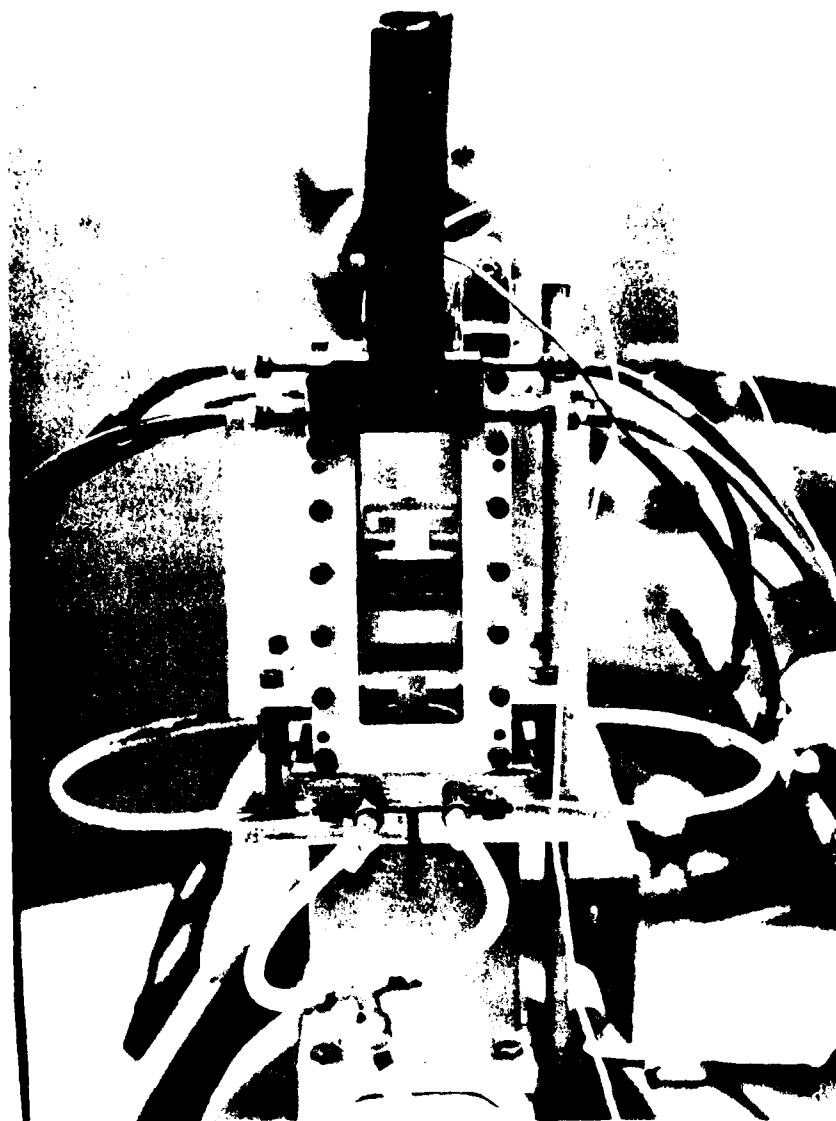


Figure 1
View of Cap Geometry, as seen from the interior of the chamber.

later. Following the fringes from the balancing chamber to the combustion chamber it is evident that outflow is occurring from both the left and right balancing chambers. The right side, in fact, appears as though a point source were located in the lower right hand corner. The flame front on the left is at the wall but on the right it is only at the centerline with a much higher gradient evident at the centerline (from the close spacing of the fringes).

In Fig. IV-5, at 30° ATDC, or 4.8 msec ATDC, the flame front moving to the right has advanced about 1 cm in 3.2 msec giving a flame speed on the order of 300 cm/sec which approximates the limiting speed for flat flame fronts⁽¹³⁾. This number has remained constant from many other optical measurements.

Penetration by the flame front is evident in the left balancing chamber while out-flow still persists in the right hand chamber. Total crank angle since spark ignition is now 42° which is about the limiting time of classical combustion⁽¹⁴⁾, this is approximately the time peak pressure is reached in the combustion chamber (from other data). Another curious observation (over many runs) is the angle of advance of the flame front with respect to the vertical direction. It is usually $15-20^\circ$ from the vertical or suggesting that the speed is faster along the clean aluminum cap surface than above it. If true, it suggests heterogeneous gas surface interaction which is faster than homogeneous gas phase reaction⁽¹⁵⁾, the activation energy for reaction being supplied by heat transfer from the cap. It should be noted that in several years of operation (for short durations) no visible deposits have been found on these caps, further attesting to the completeness of combustion and the availability of clean metallic surfaces for gas-surface interaction.

Fig. IV-6 taken at 60° ATDC or 9.66 msec ATDC shows the upper left region nearing completion of reaction while the extreme right, the region occupied by the right balancing chamber outflow in Fig. IV-5, shows strong reaction in progress. The upper cap surface shows what appears to be a center of



Figure IV-1

Two Plate Holographic Interferogram at 1000x magnification
(lower image from second reference plate, upper actual image)

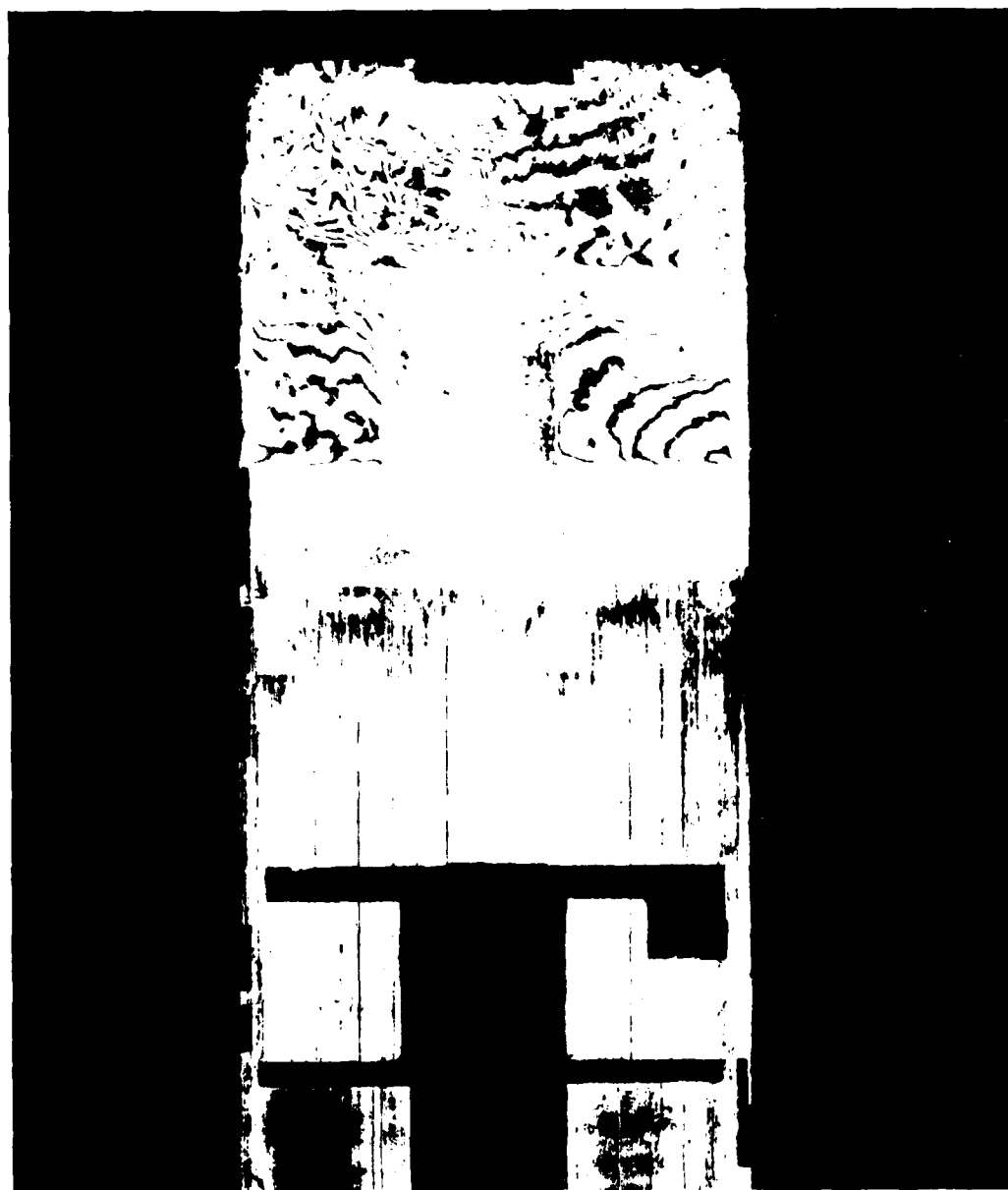


Figure IV-4

Two Plate Holographic Interferogram at 10° ATDC



Figure IV-5

Two Plate Holographic Interferogram at 30° ATDC

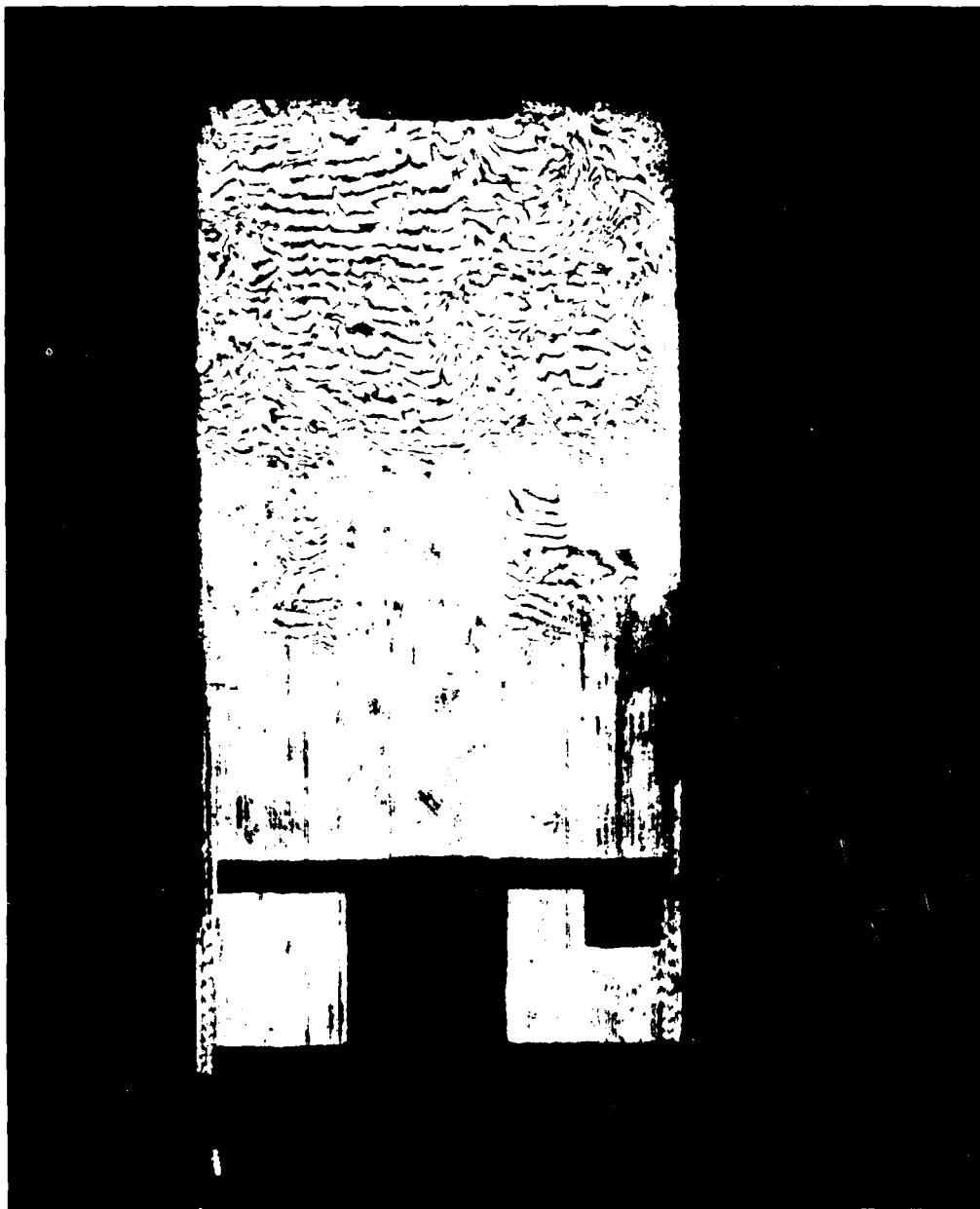


Figure IV-6

Two Plate Holographic Interferogram at 60° ATDC



Figure IV-7

Two Plate Holographic Interferogram at 80 A/D

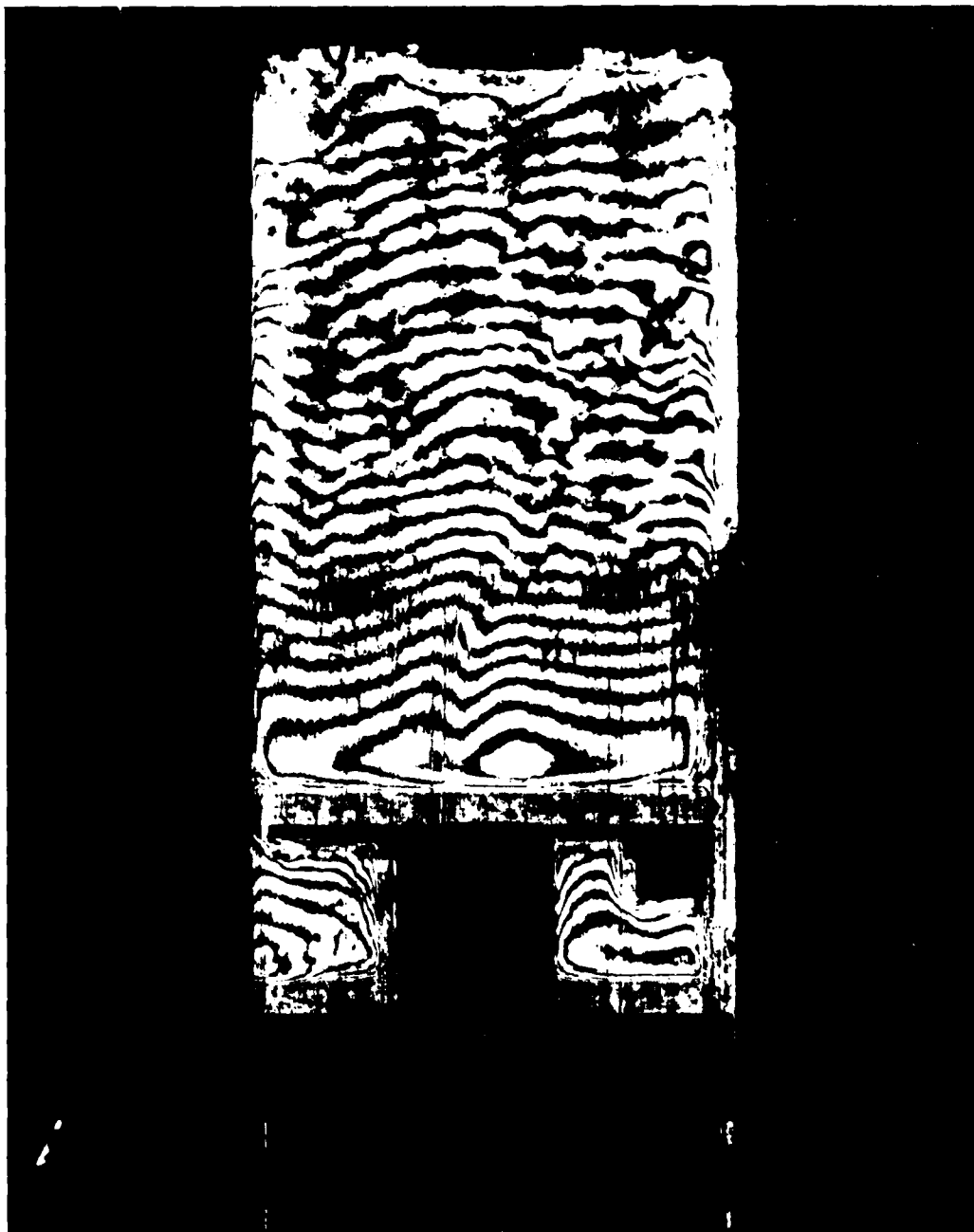


Figure IV-8

Two-Plate Holographic Interferogram at 140 ATDC

reaction just above the inner limit of the balancing chamber. Such "centers" of activity have been observed on the surface in other experiments suggesting that some surface locations may be more effective than others in promoting gas surface reaction (as in nucleation).

Inflow to the balancing chambers is clearly evident from the fringe profiles. A great difference in either concentration, temperature, or pressure (or combination thereof) exists across the boundary between the very finely spaced fringes and the wider spaced fringes in the balancing chambers.

Fig. IV-7 taken at 80° ATDC or 12.8 msec ATDC shows relatively uniform expansion in the upper region with an intense reaction zone at the lower right resulting from the admission of air and reactants from the still active right hand balancing chamber while the left hand balancing chamber is mostly inactive. Although blurred by carbon from the upper piston ring, the original negatives clearly indicate outflow from both balancing chambers.

The final photo in this series, Fig. IV-8 taken at 140° ATDC or 22.5 msec ATDC shows very little reaction, a slight outflow from the balancing chambers, and no activity in the balancing chambers.

It may prove possible at some later date to apply quantitative methods⁽¹⁶⁾ to the reduction of interferograms produced in the above manner; it is beyond the scope, however, of the present work.

V. EXPERIMENTAL OBSERVATIONS - FASTEX SCHLIEREN PHOTOGRAPHY

The same square engine described in section IV was used with a Schlieren system and 16 mm Fastex high speed camera. The light source was an Oriel Optics 500 watt Xenon lamp with a 1 mm wide vertical slit. Framing speed was about 2,400 frames per second allowing at least 72 frames for one stroke (30 ms) at 1000 RPM with ASA 400 film. The sequence shown here is typical of results observed over a period of time well over one year.

Fig. V-1 with frames 1 through 12 corresponds to ignition, a few degrees before top dead center (BTDC), to about top dead center (ATDC). The combustion kernel first evident in frame 3 grows in size until the reaction nearly fills the chamber in frame 12.

Fig. V-2 with frames 13-24 starts at about TDC and proceeds to about 5 ms after. Although a turbulent reaction has completely filled the combustion chamber, the reaction continues in spite of what appears to be interaction with the walls which were air and water cooled. Recall, however, from the interferometer results, Figs. IV-4,5, that a pulse of lean composition has by this time jetted out of the balancing chamber and formed a "curtain" around the combustion chamber. Thus the reaction is interacting with this "curtain" of lean composition which has also been heated appreciably in the balancing chamber. The temperature of this "curtain" must be in the neighborhood of auto ignition temperature since, on occasion, particles in the balancing chamber have been seen to auto ignite in color cinematography of the process. It appears the above interaction reduces classical wall quench⁽¹⁴⁾ as the reaction continues as seen in the following frames. One further note of interest is the color observed in 1/5 sec exposures of the process. The "curtain" region has a vivid blue hue while the core reaction is white.

Continuation of the reaction is seen in the first four frames of Fig. V-3; this figure covers the time interval of 5.4 to 10 ms ATDC. Frames 29 and 30

show transition to yet another time dependent reaction while the initial reaction in what was the TDC clearance volume dies out after persisting for about 11 ms. Note in frames 29 and 30 that the short gap length on the right favors early reaction while the longer one on the left tends to delay the reaction.

Proceeding on to frames 37 to 48 in Fig. V-4 from 11.4 to 15 ms ATDC, we see a much stronger reaction on the left where the long gap is located while the right side with the short gap begins to die out. This is presumably because the short length gap has not only less flow resistance but is also less effective in quenching the reaction than the long gap; thus, some of the lean mixture in the right balancing chamber was reacted by flame penetration. This is in keeping with the observations in Fig. IV-7. A rather strong outward pulse from each balancing chamber can be seen developing in frame 40 and subsequent, especially on the left.

Fig. V-5 for the time interval 15.4-20 ms ATDC shows evidence of continuing outflow from the left chamber while the reaction started in frame 29 is now more diffuse, is still stronger on the left, and exhibits a turbulence level of larger scale and is of lower intensity than before.

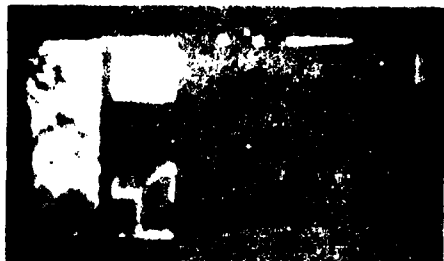
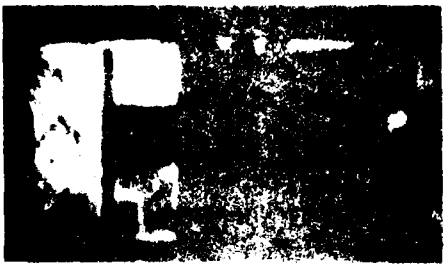
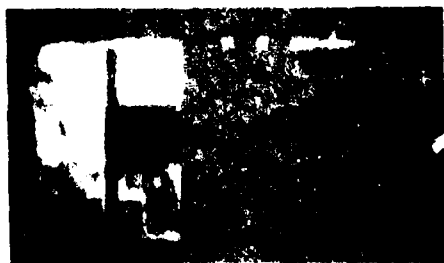
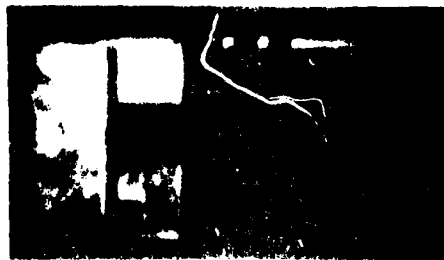
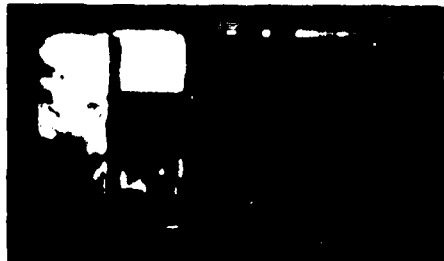
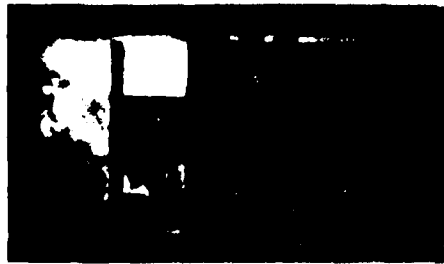
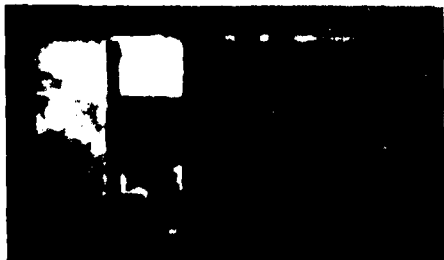
Fig. V-6 for the time interval 20.4-25 ms ATDC shows a new pulse developing as an outflow from the balancing chambers. The static-valve-lift curve for this engine shows the exhaust valve opening beginning at 40° BBDC which closely corresponds to frame 68; some outflow from the balancing chambers is observed at this point. By frame 72 valve lift is clearly evident and the pulse showing strong outflow from the balancing chambers is quite clear. The expansion wave into the cylinder created on opening of the exhaust valve creates a momentary pressure differential between the combustion chamber and balancing chamber giving rise to this outflow from the balancing chamber.

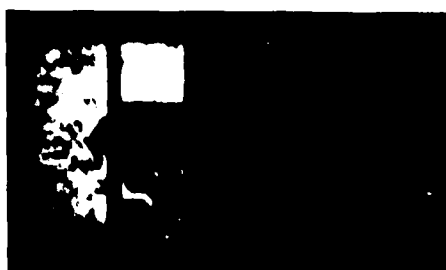
Fig. V-7 is for the time interval 25.4-30 ms ATDC. The outward pulse from

the balancing chamber is stronger yet in frame 73 and continues to increase in magnitude for the next 5 frames. By frame 79, yet another phase of reaction has developed, apparently fed by the balancing chamber outflow after opening of the exhaust valve. Although the gradients evident in these Schlieren prints appear large, color cine of the process as well as the earlier mentioned interferograms show relatively little happening. Occasional flareups are seen when carbon particles from the upper piston guide ring react.

Apparently enough energy is released in this late "clean up" reaction to generate a compression wave which accelerates the entire column of reacted gases toward the cylinder head with sufficient velocity to cause a visible rebound from the cylinder head. The velocity of the rebound first seen in frame 83 appears to be about 1.5 cm/ms, an appreciable quantity. The flow direction is, of course, opposite to outflow through the exhaust valve; this persists for about 3 to 4 ms. BDC occurs at frame 84.

Fig. V-8, all after bottom dead center, covers the time interval 30.4 to 35 ms ATDC, or 0.4 to 5 ms ABDC. The rebound process first observed in Fig. V-7 is quite clear now and quite dramatic in slow motion cine. It persists long enough to interact with the weak reaction that originated in the vicinity of the cap and late in the exhaust stroke (not shown) creates a highly turbulent final cylinder reaction which is then exhausted from the cylinder. Also evident is a return flow into the balancing chamber which originates in Fig. V-7, frame 82 and becomes quite strong by frame 96 in this figure. The pressure imbalance between chambers that causes this final inflow is due to the compression wave generated by the final chemical reaction originating in frame 79 as well as the fluid inertia as the piston starts upward after BDC.





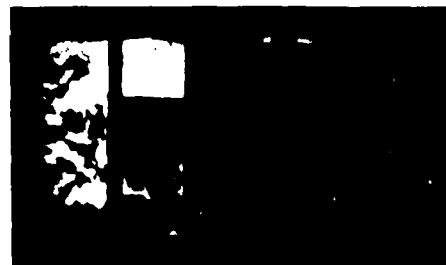
18



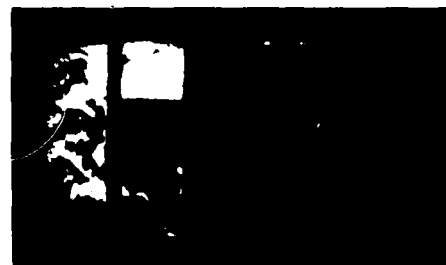
17



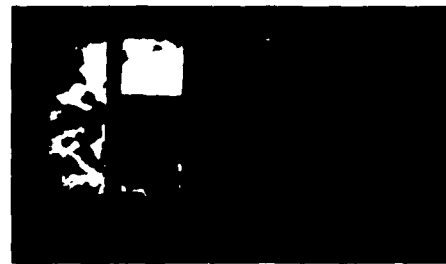
16



15



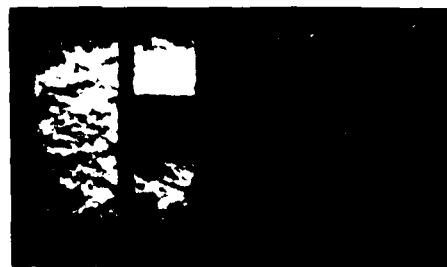
14



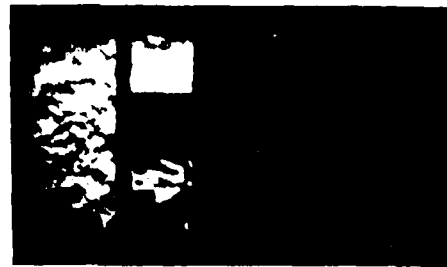
13



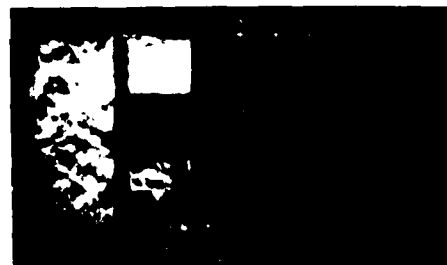
24



23



22



21



20



19

Figure V-2

Eastex Schlieren Photos, 100 to 5 msec.



30



29



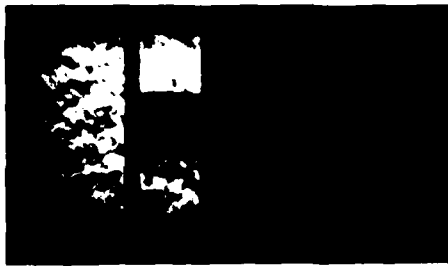
28



27



26



25



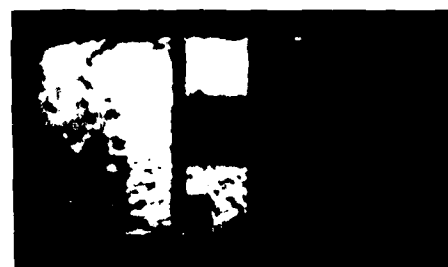
36



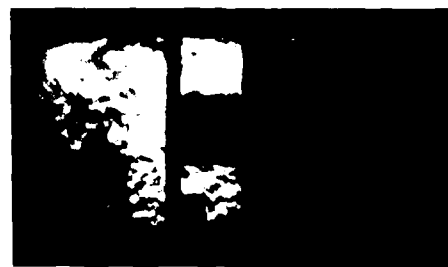
35



34



33



32



31

Figure V-3

Eastex Schlieren Photos, 0.4 to 10 msec, ATD

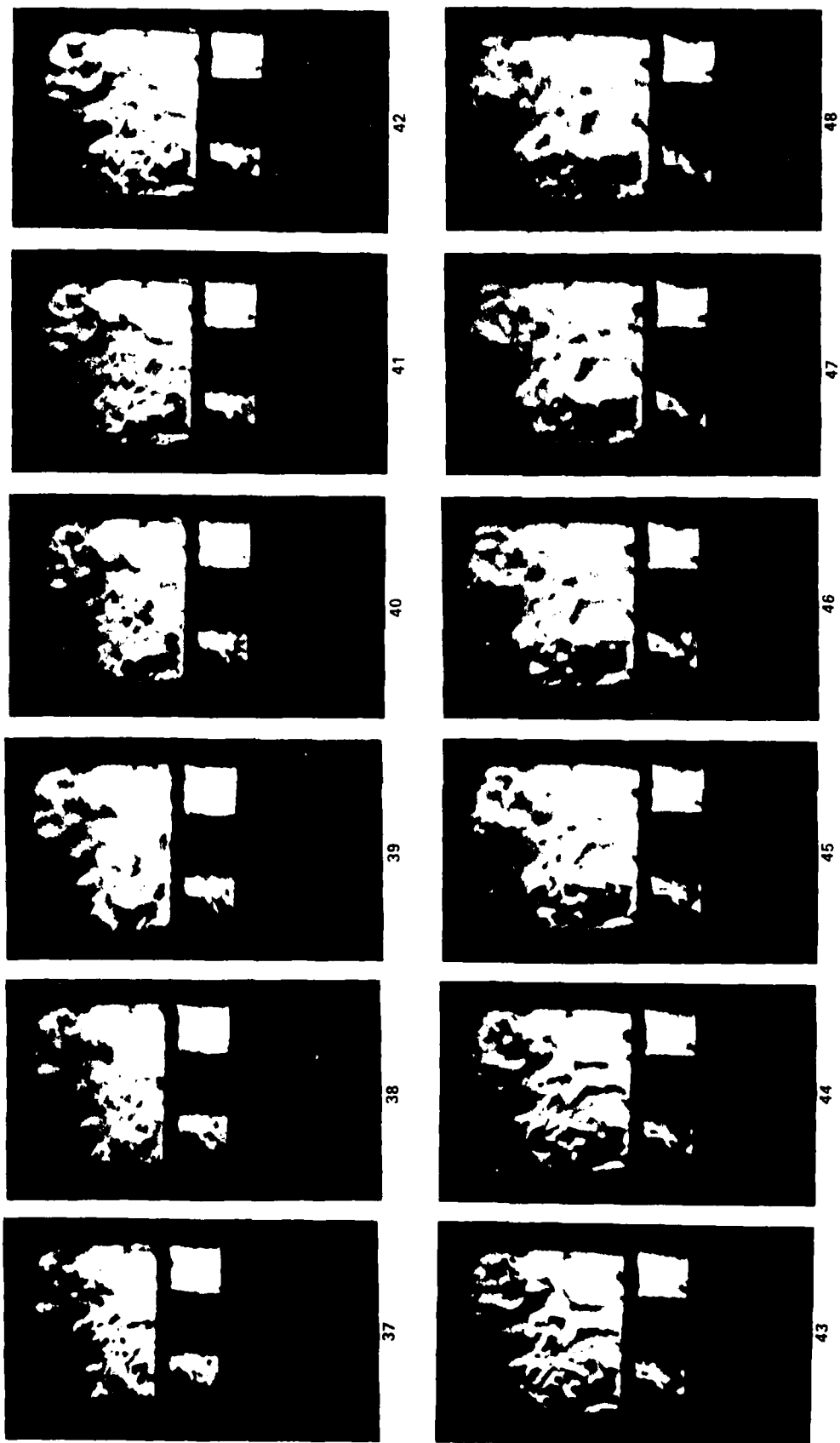


Figure V-4

Fastex Schlieren Photos, 11.4 to 15 msec. ATDC



54



53



52



51



50



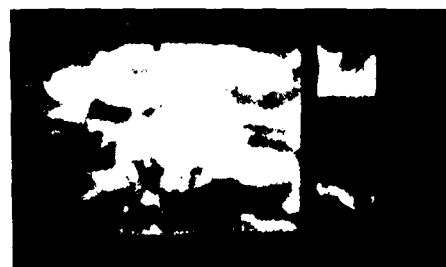
49



60



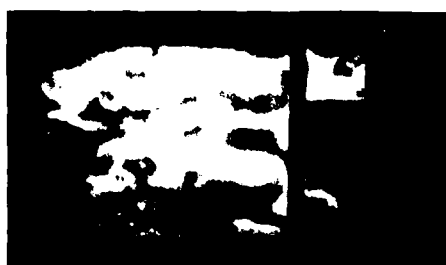
59



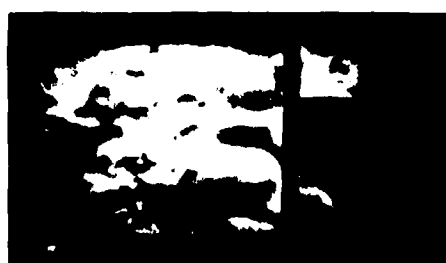
58



57



56



55

Figure V-5

Fastex Schlieren Photos, 15.4 to 20 msec. ATDC



66



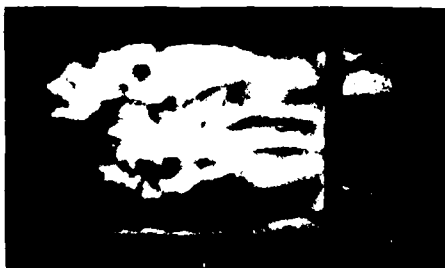
72



65



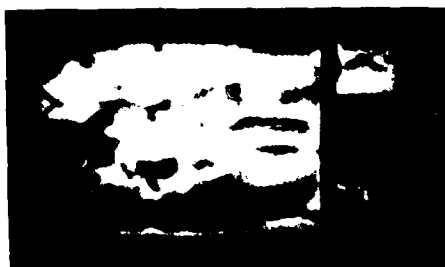
71



64



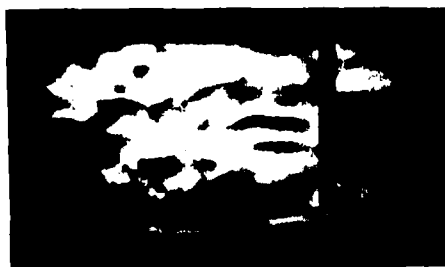
70



63



69



62



68



61



67

Figure V-6

Fastex Schlieren Photos, 20.4 to 25 msec. ATDC



78



84



77



83



76



82



75



81



74



80



73



79

Figure V-7

Fastex Schlieren Photos, 25.4 to 30 msec. ATDC



90



96



89



95



88



94



87



93



86



92



85



91

Figure V-3

Fastex Schlieren Photos, 30.4 to 35msec. ATD

VI. CONCLUSIONS

1. One dimensional non-steady gasdynamics, even for the simplified model reviewed here, does confirm the existence of flow reversal in the first millisecond with short duration outflow from the balancing chamber to the combustion chamber while the average pressure in the combustion chamber is increasing with time; continuation of the calculation to later times should be facilitated by the supporting optical observations presented here.
2. Fastex Schlieren photography and holographic interferometry are useful for qualitative analysis of time dependent combustion processes and some quantitative measurements are possible.
3. Gap length is important in quenching of the combustion reaction and controlling reaction rates.
4. Time dependent combustion with pressure exchange and attendant mass transport can be used to control the pressure-temperature time history of reaction; extension of the non-steady theory should allow optimization of the geometries involved.
5. At least four macromodes of combustion can be identified in this type of engine and are summarized in Table VI-1 and Fig. VI-1.

TABLE VI-1
MACROMODES OF COMBUSTION

Mode	Description
I	Initial rapid rate of reaction, in essentially IDC combustion chamber volume, wave compression in balancing chamber, mass transport to combustion chamber.
II	Prolongation of initial reaction with oxygen supplied by mass transport from balancing chamber.
IIIa	Mode III probably due to combined effects; secondary wave reflections, heat transfer to balancing chamber gases plus possible radical formation in hot balancing chamber, all providing the means for further mass transport to the combustion chamber.
IIIb,c	Continuation of Mode III, with a short length clearance gap favoring early reaction, a long length favoring late reaction.
IV	Final mode with balancing chamber purge due to strong expansion wave from exhaust valve opening, mostly non-luminous reaction, some extremely luminous reaction when carbon particles, other combustibles encounter oxygen exiting balancing chambers. Reaction apparently strong enough to initiate compression wave accelerating displacement volume upward and rebounding from cylinder head.

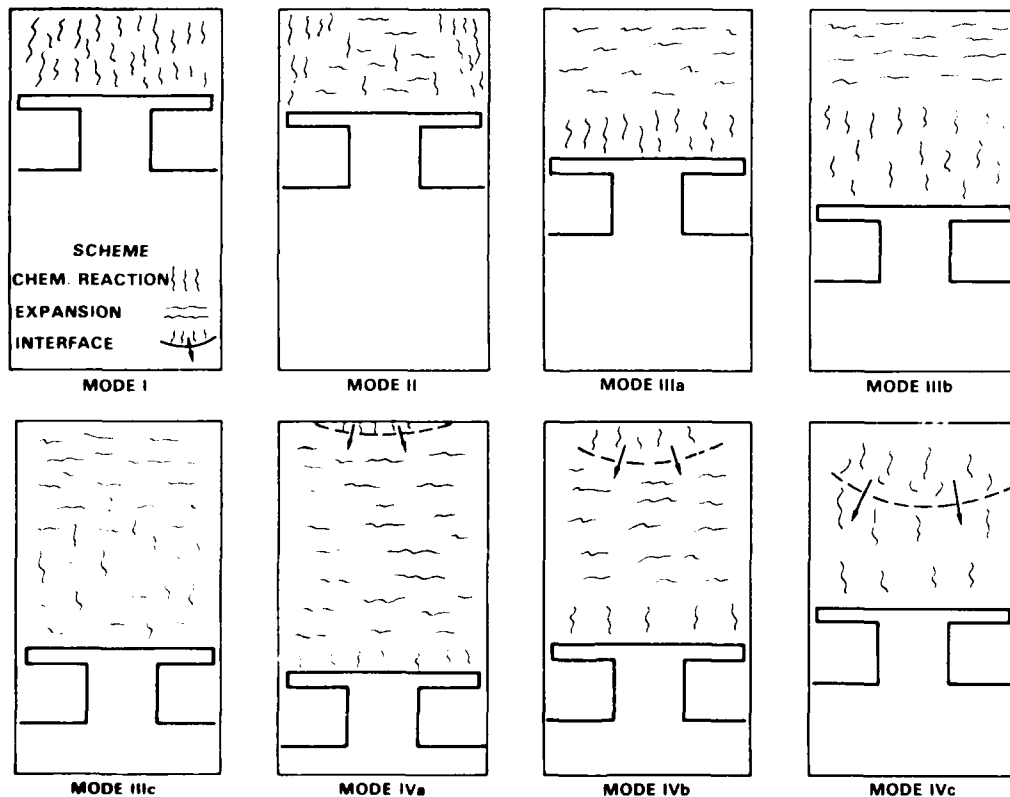


FIGURE VI-1
MACROMODE OF TIME DEPENDENT COMBUSTION

REFERENCES

1. Blaser, R. F., Ph.D. Thesis Research Proposal, 1974 (to be published)
2. Keating, E. L., Blaser, R. F., and Pouring, A. A., Quasi-Equilibrium Air Standard Heat Balanced Cycle Analysis, SAE Paper #789036, August, 1978.
3. Pouring, A. A., Blaser, R. F., Keating, E. L., and Rankin, B. H., The Influence of Combustion with Pressure Exchange on the Performance of Heat Balanced Internal Combustion Engines, S.A.E. Paper 770120, February, 1977.
4. Pandalai, R. P., Preliminary Investigation of the Nonsteady Combustion and Flow Processes of the Naval Academy Heat Balanced Engine (NAHBE), USNA, Engineering and Weapons Report EW-10-78, May, 1978.
5. Keating, E. L. and Pouring, A. A., Quasi-Equilibrium Fuel-Air Heat Balanced Cycle Analysis, USNA Engineering and Weapons Report EW-14-79, November, 1979.
6. Anonymous, Stratified Charge Engines, I. Mech. E. Conference Publication 1976-11, Institute of Mechanical Engineers, London, 1977.
7. Mattavi, J. N. and Amann, C. A., Combustion Modeling in Reciprocating Engines, Plenum Press, New York, 1980.
8. Whited, T. L., Performance Analysis of a Modified Internal Combustion Engine, Report No. USNA-TSPR-90, May 1977, AD No. AD45378.
9. Brastauskas, J. P., Time Dependent Film Analysis of the NAHBE Combustion Process Utilizing Schlieren Techniques, AIAA Student Conference, U. S. Naval Academy, April 1980.
10. Foa, J. V., Elements of Flight Propulsion, John Wiley, New York, 1960.
11. Rudinger, G., Wave Diagrams for Nonsteady Flow, Van Nostrand, New York, 1955.
12. Hannah, B. W. and King, W. L. Jr., Extensions of Dual-Plate Holographic Interferometry, AIAA 9th Aerodynamic Testing Conference, Arlington, Texas, June 1976 (see also International Congress on Instrumentation in Aerospace Simulation Facilities, Ottawa, Canada, September 1975).
13. Fristrom, R. M., Westenberg, A. A., Flame Structure, McGraw-Hill, New York, 1965.
14. Patterson, D. J., Henein, N. A., Emissions from Combustion Engines and their Control, Ann Arbor Science Publishers, Ann Arbor, Michigan, 1972.
15. Hinshelwood, C. N., The Kinetics of Chemical Change in Gaseous Systems, Oxford, 1933.
16. Weinberg, F. J., Optics of Flames, Butterworths, 1963.

DAT
ILM